

1 **Astrocyte Ca²⁺ Signaling is Facilitated in an *Scn1a*^{+/-}** 2 **Mouse Model of Dravet Syndrome**

3
4 **Kouya Uchino¹, Wakana Ikezawa¹, Yasuyoshi Tanaka² Masanobu Deshimaru²,**
5 **Kaori Kubota¹, Takuya Watanabe¹, Shutaro Katsurabayashi^{1,2,*}, Katsunori**
6 **Iwasaki^{1,*} and Shinichi Hirose^{2,3,*}**

7
8 ¹Department of Neuropharmacology, Faculty of Pharmaceutical Sciences, Fukuoka
9 University, Fukuoka, Japan

10 ²Research Institute for the Molecular Pathogenesis of Epilepsy, Fukuoka University,
11 Fukuoka, Japan

12 ³General Medical Research Center, School of Medicine, Fukuoka University, Fukuoka,
13 Japan.

14 ***Correspondence:**

15 Shutaro Katsurabayashi, Ph.D.
16 shutarok@fukuoka-u.ac.jp

17
18 Katsunori Iwasaki, Ph.D.
19 iwasakik@fukuoka-u.ac.jp

20
21 Shinichi Hirose, M.D., Ph.D.
22 hirose@fukuoka-u.ac.jp

23
24
25
26
27 **Running title:** Ca²⁺ spiking in DS astrocyte

28
29 **No. of words:** 1786

30 **No. of figures:** 2

31 **No. of tables:** 0

32

33

Contribution to the field

Dravet syndrome (DS) usually begins in the first year of life and is a severe form of epilepsy that often leads to severe encephalopathy. Over 80% of DS patients have a heterozygous mutation in *SCN1A* (which encodes a subunit of voltage-gated Na⁺ channels). However, the mechanisms underlying this disease remain unknown, which makes drug development difficult.

In addition to neuronal involvement, astrocytes—the most abundant glial cell type in the brain—are also involved in the pathogenesis of epilepsy. Therefore, astrocytes are attracting attention as a new therapeutic target for epilepsy. In this study, we found that Ca²⁺ spiking was significantly faster and that ATP-induced Ca²⁺ spiking was more significant in astrocytes cultured from *Scn1a*^{+/-} mice compared with that in astrocytes from wild-type mice.

This paper demonstrates that Ca²⁺ dynamics in astrocytes may be involved in the pathogenesis of DS. Astrocytes play a vital role in protecting neural circuits; therefore, the changes we identified in *Scn1a*^{+/-} astrocyte Ca²⁺ signaling may help in the development of novel therapies for epilepsy that target astrocytes to protect neural circuits.

Abstract

Dravet syndrome (DS) is an infantile-onset epileptic encephalopathy. More than 80% of DS patients have a heterozygous mutation in *SCN1A*, which encodes a subunit of the voltage-gated sodium channel, Nav_{1.1}, in neurons. The roles played by astrocytes, the most abundant glial cell type in the brain, have been investigated in the pathogenesis of epilepsy; however, the specific involvement of astrocytes in DS has not been clarified. In this study, we evaluated Ca²⁺ signaling in astrocytes using genetically modified mice that have a loss-of-function mutation in *Scn1a*. We found that the slope of spontaneous Ca²⁺ spiking was increased without a change in amplitude in *Scn1a*^{+/-} astrocytes. In addition, ATP-induced transient Ca²⁺ influx and the slope of Ca²⁺ spiking were also increased in *Scn1a*^{+/-} astrocytes. These data indicate that perturbed Ca²⁺ dynamics in astrocytes may be involved in the pathogenesis of DS.

Keywords: epilepsy, Dravet syndrome, *Scn1a*, astrocyte, Ca²⁺

68

69 Introduction

70 Epilepsy is a chronic neurological disorder that causes paroxysmal loss of
 71 consciousness and convulsions because of overexcitement of neurons in the brain (1).
 72 Antiepileptic drugs are commonly used to treat epilepsy, but 20%–30% of patients show
 73 resistance to drug therapy (2). Dravet syndrome (DS) is an epileptic encephalopathy that
 74 occurs in infancy at a frequency of 1 in 20,000 to 40,000 children (3, 4). In addition,
 75 70%–80% of DS patients have heterozygous mutations in sodium voltage-gated channel
 76 alpha subunit 1 (*SCN1A*), which encodes a subunit of the voltage-gated sodium channel,
 77 Nav_{1.1} (5). A mouse model with a heterozygous loss-of-function mutation in *Scn1a* was
 78 recently reported as a DS model (6–9). We recently reported that the excitatory and
 79 inhibitory balance of synaptic transmission was disrupted in heterozygous *Scn1a*
 80 knockin (*Scn1a*^{+/-}) mouse neurons when the extracellular Ca²⁺ concentration was
 81 increased (10). The above studies show that mutations in the *Scn1a* gene cause
 82 abnormal neurological function. In addition to neuronal dysfunction, the involvement of
 83 glial cells in the pathogenesis of epilepsy has also been suggested (11). In particular,
 84 astrocytes, a type of glial cell, are involved in epilepsy pathogenesis by regulating
 85 neurotransmitter and ion concentrations (12). Therefore, astrocytes are a promising new
 86 therapeutic target for epilepsy.

87 Unlike neurons, which transmit information by generating action potentials,
 88 astrocytes do not generate action potentials and have been considered non-excitabile
 89 cells. However, astrocytes are found throughout the central nervous system and play an
 90 essential role in neuronal function (13). For example, we have demonstrated that the
 91 long-term culture of astrocytes and changes in astrocyte density can alter neuronal
 92 growth and synaptic transmission (14, 15). Advances in Ca²⁺ imaging methods have
 93 revealed that astrocytes are excitable cells that exhibit intracellular Ca²⁺ signaling (16).
 94 Astrocytes regulate neuronal activity by releasing glial transmitters and
 95 neurotransmitters, such as glutamate, ATP, and D-serine (17). In addition, astrocyte Ca²⁺
 96 signaling is involved in epileptic seizures via neurons (18, 19). *Scn1a* mutations change
 97 the neuronal expression of Ca²⁺ channels and sensitivity to Ca²⁺ (10, 20); however, it is
 98 not known if astrocytes are affected in the DS model. In this study, we evaluated Ca²⁺
 99 dynamics in astrocytes using genetically modified *Scn1a*^{+/-} mice.

100

101 Materials and Methods

102 **Animals**

103 Experimental animals were handled in accordance with the ethical regulations for
104 animal experiments of the Fukuoka University Experimental Animal Care and Use
105 Committee. All animal protocols were approved by the Ethics Committee of Fukuoka
106 University (permit numbers: 1712128 and 1812092). All experimental protocols were
107 performed according to the relevant guidelines and regulations of Fukuoka University.
108 All *in vivo* work was carried out in compliance with ARRIVE guidelines. *Scn1a*^{+/-} mice,
109 in which coding exons 8–12 of *Scn1a* were replaced with a neomycin resistance gene,
110 were generated as previously described (10). The mice were housed in plastic cages and
111 kept at 23±2°C, in 60±2% humidity, and with a 12-hour light/dark cycle (lights on at
112 7:00 am, lights off 7:00 pm). Food (CE-2, CLEA Japan, Inc., Tokyo, Japan) and water
113 were freely available.

115 **Astrocyte culture**

116 For astrocyte culture, newborn *Scn1a*^{+/-} mice (P0–1) were used. Tail biopsies were
117 taken and PCR performed to confirm the *Scn1a* genotype (10). Cerebral cortices of
118 0–1-day-old mice were treated with trypsin/EDTA (0.05%/0.02%) and cultured in
119 D-MEM medium containing 10% fetal bovine serum at 37°C for 2 weeks. The astrocyte
120 layer adhering to the bottom of the culture bottle was then detached with trypsin/EDTA
121 (0.05%/0.02%). Cultured astrocytes were seeded at a density of 75,000 cells/well in
122 six-well plates on glass coverslips coated with collagen/poly-D-lysine and cultured for
123 7–8 days.

125 **Ca²⁺ imaging**

126 Spontaneous Ca²⁺ signaling was monitored using Oregon-Green BAPTA-1 AM, a
127 fluorescent Ca²⁺ indicator (Thermo Fisher Scientific, Waltham, MA, USA).
128 Oregon-Green BAPTA-1 AM emits green fluorescence at resting Ca²⁺ levels, and the
129 fluorescence intensity increases with increasing Ca²⁺ binding. ATP-induced Ca²⁺
130 signaling was monitored using Fluo4-AM, a fluorescent Ca²⁺ indicator that does not
131 have a resting signal (Thermo Fisher Scientific). Fluo4-AM shows minimal
132 fluorescence at resting Ca²⁺ levels, and the fluorescence emission intensity increases
133 with Ca²⁺ binding.

134 Astrocytes were incubated with Oregon-Green BAPTA-1, AM, or Fluo4-AM for
135 60 min. Astrocytes were incubated with NucBlue (Thermo Fisher Scientific) for 20 min
136 to identify nuclei. The glass coverslips were then transferred to a recording chamber and
137 refluxed with an extracellular solution. Fluorescence excitation was performed using

LED (light-emitting diode) irradiation (Lambda HPX, Sutter Instrument, Novato, CA, USA). For time-lapse imaging, the LED flash and the exposure time of an sCMOS camera (edge4.2, pco, Kelheim, Germany) were synchronized. Oregon-Green BAPTA-1, AM was irradiated with 494 nm excitation light and observed with a fluorescence wavelength of 523 nm (exposure time 100 ms, interval 1000 ms, number of images 360). Fluo4-AM was irradiated with 495 nm excitation light and observed with a fluorescence wavelength of 518 nm (exposure time 100 ms, interval 1000 ms, number of images 360). For Fluo4-AM observation, 1 μ M ATP was applied for 30 s to induce Ca^{2+} signaling.

Data analysis

ImageJ software (1.53c, Wayne Rasband, NIH, USA) and AxoGraph X software (1.2, AxoGraph Scientific, Sydney, Australia) were used to analyze the dynamics of Ca^{2+} signaling. Images stained with NucBlue were divided into nuclei and background by threshold; a unit of >100 pixels was considered the location of a nucleus and registered as a region of interest (ROI). The ROIs were then fitted to the stacked images, and the intensity change was measured. The maximum intensity value in the stack image for each nucleus was transferred to Axograph. For analysis of spontaneous Ca^{2+} signaling, the data value was relativized in Axograph, and the maximum relative intensity was calculated. The data were differentiated from the relative value, and the maximum differential intensity was obtained. For analysis of ATP-induced Ca^{2+} signaling, the intensity (F) of each ROI was normalized by the intensity before ATP application (F0). The area under the curve (AUC) of intensity was also measured from the ATP-induced Ca^{2+} wave. In addition, the F/F0 was differentiated, and the maximum differential intensity was calculated.

Solutions

Extracellular solution (pH 7.4) consisted of (mM): NaCl 140, KCl 2.4, HEPES 10, glucose 10, CaCl_2 2, and MgCl_2 1. ATP (Thermo Fisher Scientific) was dissolved in ultrapure water to make a 100-mM stock solution. The stock was diluted in extracellular solution to 1 μ M just before use.

Statistics

All data are expressed as the mean \pm standard error. A lowercase n indicates the number of astrocytes recorded, and an uppercase N indicates the number of cultures (lot number). Two groups were compared with Student's unpaired t-test using Kaleida Graph 3.6 (Synergy Software, Reading, PA, USA). Statistical significance was

174 considered when $p < 0.05$.

175

176 Results

177 Astrocytes regulate neurotransmitter and ion concentrations in neurons and other glial
178 cells via Ca^{2+} signaling. The concentrations of many neurotransmitters and ions are
179 abnormal in epilepsy; therefore, we expected that Ca^{2+} signaling would be altered in
180 *Scn1a*^{+/-} astrocytes. Oregon-Green BAPTA-1, AM detects the resting signal of Ca^{2+} ,
181 meaning that it was not possible to fix a baseline or to measure the frequency of
182 spontaneous Ca^{2+} spiking because of baseline instability. Therefore, we first obtained
183 the relative strength of spontaneous Ca^{2+} signaling in cultured astrocytes from the
184 cerebral cortex of *Scn1a*^{+/-} mice. The maximum relative intensity of spontaneous Ca^{2+}
185 signaling was identical between wild-type (WT) and *Scn1a*^{+/-} astrocytes (Figures 1A, B,
186 C). To analyze the Ca^{2+} waveform in more detail, we differentiated the waveform of
187 spontaneous Ca^{2+} signaling. As a result, the maximum differential intensity was
188 significantly increased in *Scn1a*^{+/-} compared with WT astrocytes (Figures 1D, E). These
189 results indicate that the unitary speed of Ca^{2+} spiking was increased without change in
190 the amount of spontaneous Ca^{2+} influx in *Scn1a*^{+/-} astrocytes.

191 In epilepsy, external stimuli may trigger neuronal hyperexcitability, resulting in
192 epileptic seizures. Therefore, we stimulated astrocytes with ATP (1 μM) and recorded
193 the ATP-induced Ca^{2+} signaling. As shown in Figure 2, the maximum peak intensity was
194 dramatically increased in *Scn1a*^{+/-} astrocytes (Figures 2A, B, C). However, there was no
195 significant difference in the AUC of ATP-induced Ca^{2+} signaling between WT and
196 *Scn1a*^{+/-} astrocytes (Figure 2D). These data indicate that *Scn1a*^{+/-} astrocytes exhibit a
197 sharper Ca^{2+} waveform. We then analyzed the slope of the wave by differentiating the
198 Ca^{2+} waveform and, as expected, the maximum differential intensity significantly
199 increased in *Scn1a*^{+/-} astrocytes (Figures 2E, F). These results indicate that the transient
200 dynamics of Ca^{2+} spiking by ATP stimulation were facilitated without changing the total
201 amount of Ca^{2+} signaling in *Scn1a*^{+/-} astrocytes.

202

203 Discussion

204 Astrocytes regulate the concentrations of neurotransmitters and ions in neurons and
205 other glial cells via Ca^{2+} signaling. The concentrations of many neurotransmitters and
206 ions are abnormal in epilepsy (21); therefore, we expected that Ca^{2+} signaling in
207 astrocytes would be disrupted in the DS mouse model. Our results show that the

transient spontaneous influx of Ca^{2+} did not change, but that the slope of Ca^{2+} spiking increased in *Scn1a*^{+/-} astrocytes. Likewise, in response to ATP stimulation, there was no change in the total amount of Ca^{2+} signaling, but the transient Ca^{2+} influx and the slope of Ca^{2+} spiking increased in *Scn1a*^{+/-} astrocytes. These results indicate that Ca^{2+} signaling is somehow enhanced in *Scn1a*^{+/-} astrocytes. Spontaneous Ca^{2+} signaling in astrocytes is thought to result from the uptake of extracellular Ca^{2+} . In contrast, stimulus-induced Ca^{2+} signaling is thought to be caused by the release of Ca^{2+} into the endoplasmic reticulum via the activation of Gq protein-coupled receptors (17). In the present study, both spontaneous and ATP-induced Ca^{2+} signaling were enhanced in *Scn1a*^{+/-} astrocytes, indicating that the function of both cascades may be enhanced.

Since it was first reported that the concentration of cytoplasmic Ca^{2+} in cultured astrocytes increases in response to glutamate (22), the concept of electrically unresponsive astrocytes sensing glutamate transmission has been accepted. This observation, and that the increase in astrocyte Ca^{2+} is associated with neurotransmitter release, is the basis for the concept of tripartite synapses (23–25). Astrocytes release glutamate via metabotropic glutamate receptors (mGluRs), which is thought to regulate the amount of glutamate in the brain, although this is a controversial assumption (26, 27). The expression of mGluRs in astrocytes is increased in mouse models of epilepsy (28), indicating that mGluR activation contributes to epileptic seizures caused by excess glutamate release in the brain (29). However, ATP released upon Ca^{2+} signaling is degraded to adenosine; therefore, adenosine may suppress epileptic seizures by exerting an inhibitory effect on neurons through pre-synaptic A1 receptors (30).

In conclusion, it is not known whether enhanced astrocyte Ca^{2+} signaling exacerbates epileptic seizures or suppresses them. However, the present study indicates that astrocytes are involved in the pathogenesis of DS. This may lead to novel pharmaceutical treatments that target non-traditional mechanisms. We suggest that study of the interaction between astrocytes and neurons, focusing on the clinical context in humans, is warranted.

Acknowledgements

We thank the members of our laboratory for their assistance. We thank Jeremy Allen, PhD, from Edanz (<https://jp.edanz.com/ac>) for editing a draft of this manuscript.

Data Availability Statement

242 The data included in this study are available from the corresponding author on
243 reasonable request.

244

245 **Ethics Statement**

246 We confirm that we have read the Journal's position on issues involved in ethical
247 publication and affirm that this report is consistent with these guidelines.

248

249 **Author Contributions**

250 K.U., W.I. and Y.T. performed experiments and analyzed data; Y.T. and M.D. created the
251 *Scn1a*^{+/-} mouse model; S.K. conceived the study; K.K., T.W., K.I., and S.H. interpreted
252 the data; K.U. and S.K. wrote the manuscript with input from all authors. All authors
253 reviewed the manuscript.

254

255 **Funding**

256 This work was supported by a KAKENHI Grant-in-Aid for Scientific Research (C) to
257 S.K. (No. 17K08328) from the Japan Society for the Promotion of Science, and the
258 Science Research Promotion Fund and The Fukuoka University Fund to S.H. (Nos.
259 G19001 and G20001), a grant for Practical Research Project for Rare/Intractable
260 Diseases from the Japan Agency for Medical Research and development (AMED) to
261 S.H. (Nos. 15ek0109038h0002 and 16ek0109038h0003), a KAKENHI Grant-in-Aid for
262 Scientific Research (A) to S.H. (No. 15H02548), a KAKENHI Grant-in-Aid for
263 Scientific Research (B) to S.H. (Nos. 20H03651, 20H03443 and 20H04506), the
264 Acceleration Program for Intractable Diseases Research utilizing Disease-specific iPS
265 cells from AMED to S.H. (Nos. 17bm0804014h0001, 18bm0804014h0002, and
266 19bm0804014h0003), a Grant-in-Aid for the Research on Measures for Intractable
267 Diseases to S.H. (H31-Nanji-Ippan-010), the Program for the Strategic Research
268 Foundation at Private Universities 2013-2017 from the Ministry of Education, Culture,
269 Sports, Science, and Technology (MEXT) to S.H. (No. 924), and the Center for Clinical
270 and Translational Research of Kyushu University Hospital to S.H. (No. 201m0203009
271 j0004).

272

273 **Conflict of Interest**

274 None of the authors has any conflict of interest to disclose.

275

276 **References**

- 277 1. Fisher RS, Acevedo C, Arzimanoglou A, Bogacz A, Cross JH, Elger CE, et al.
278 ILAE official report: a practical clinical definition of epilepsy. *Epilepsia* (2014)
279 55(4):475-82. doi: 10.1111/epi.12550
280
- 281 2. Dalic L, Cook MJ. Managing drug-resistant epilepsy: challenges and solutions.
282 *Neuropsychiatr Dis Treat* (2016) 12:2605-2616. doi: 10.2147/NDT.S84852
283
- 284 3. Brunklaus A, Ellis R, Reavey E, Forbes GH, Zuberi SM. Prognostic, clinical and
285 demographic features in SCN1A mutation-positive Dravet syndrome. *Brain* (2012)
286 135(Pt 8):2329-36. doi: 10.1093/brain/aww151.
287
- 288 4. Bayat A, Hjalgrim H, Møller RS. The incidence of SCN1A-related Dravet
289 syndrome in Denmark is 1:22,000: a population-based study from 2004 to 2009.
290 *Epilepsia* (2015) 56(4):e36-9. doi: 10.1111/epi.12927.
291
- 292 5. Connolly MB. Dravet Syndrome: Diagnosis and Long-Term Course. *Can J Neurol*
293 *Sci* (2016) Suppl 3:S3-8. doi: 10.1017/cjn.2016.243
294
- 295 6. Yu FH, Mantegazza M, Westenbroek RE, Robbins CA, Kalume F, Burton KA, et al.
296 Reduced sodium current in GABAergic interneurons in a mouse model of severe
297 myoclonic epilepsy in infancy. *Nat Neurosci* (2006) 9(9):1142-9. doi:
298 10.1038/nm1754
299
- 300 7. Ogiwara I, Miyamoto H, Morita N, Atapour N, Mazaki E, Inoue I, et al. Nav_{1.1}
301 localizes to axons of parvalbumin-positive inhibitory interneurons: a circuit basis
302 for epileptic seizures in mice carrying an Scn1a gene mutation. *J Neurosci* (2007)
303 27(22):5903-14. doi: 10.1523/JNEUROSCI.5270-06.2007
304
- 305 8. Cheah CS, Yu FH, Westenbroek RE, Kalume FK, Oakley JC, Potter GB, et al.
306 Specific deletion of Nav_{1.1} sodium channels in inhibitory interneurons causes
307 seizures and premature death in a mouse model of Dravet syndrome. *Proc Natl*
308 *Acad Sci U S A* (2012) 109(36):14646-51. doi: 10.1073/pnas.1211591109

- 309
- 310 9. Han S, Tai C, Westenbroek RE, Yu FH, Cheah CS, Potter GB, et al. Autistic-like
- 311 behaviour in *Scn1a*^{+/-} mice and rescue by enhanced GABA-mediated
- 312 neurotransmission. *Nature* (2012) 489(7416):385-90. doi: 10.1038/nature11356
- 313
- 314 10. Uchino K, Kawano H, Tanaka Y, Adaniya Y, Asahara A, Deshimaru M, et al.
- 315 Inhibitory Synaptic Transmission Is Impaired at Higher Extracellular Ca²⁺
- 316 Concentrations in *Scn1a*^{+/-} Mouse Model of Dravet Syndrome. *Sci Rep* (2021) *in*
- 317 *press*.
- 318
- 319 11. Patel DC, Tewari BP, Chaunsali L, Sontheimer H. Neuron-glia interactions in the
- 320 pathophysiology of epilepsy. *Nat Rev Neurosci* (2019) 20(5):282-297. doi:
- 321 10.1038/s41583-019-0126-4
- 322
- 323 12. Coulter DA, Steinhäuser C. Role of astrocytes in epilepsy. *Cold Spring Harb*
- 324 *Perspect Med* (2015) 5(3):a022434. doi: 10.1101/cshperspect.a022434
- 325
- 326 13. Allen NJ, Barres BA. Neuroscience: Glia - more than just brain glue. *Nature* (2009)
- 327 457(7230):675-7. doi: 10.1038/457675a
- 328
- 329 14. Kawano H, Katsurabayashi S, Kakazu Y, Yamashita Y, Kubo N, Kubo M, et al.
- 330 Long-term culture of astrocytes attenuates the readily releasable pool of synaptic
- 331 vesicles. *PLoS One* (2012) 7(10):e48034. doi: 10.1371/journal.pone.0048034
- 332
- 333 15. Oyabu K, Takeda K, Kawano H, Kubota K, Watanabe T, Harata NC, et al.
- 334 Presynaptically silent synapses are modulated by the density of surrounding
- 335 astrocytes. *J Pharmacol Sci* (2020) 144(2):76-82. doi: 10.1016/j.jphs.2020.07.009
- 336
- 337 16. de Melo Reis RA, Freitas HR, de Mello FG. Cell Calcium Imaging as a Reliable
- 338 Method to Study Neuron-Glial Circuits. *Front Neurosci* (2020) 14:569361. doi:
- 339 10.3389/fnins.2020.569361.
- 340
- 341 17. Agulhon C, Petravic J, McMullen AB, Sweger EJ, Minton SK, Taves SR, et al.
- 342 What is the role of astrocyte calcium in neurophysiology? *Neuron* (2008)
- 343 59(6):932-46. doi: 10.1016/j.neuron.2008.09.004
- 344

- 345 18. Tian GF, Azmi H, Takano T, Xu Q, Peng W, Lin J, et al. An astrocytic basis of
346 epilepsy. *Nat Med* (2005) 11(9):973-81. doi: 10.1038/nm1277
347
- 348 19. Fellin T, Gomez-Gonzalo M, Gobbo S, Carmignoto G, Haydon PG. Astrocytic
349 glutamate is not necessary for the generation of epileptiform neuronal activity in
350 hippocampal slices. *J Neurosci* (2006) 26(36):9312-22. doi:
351 10.1523/JNEUROSCI.2836-06.2006
352
- 353 20. Shi X, He W, Guo S, Zhang B, Ren S, Liu K, Sun T, Cui J. RNA-seq Analysis of
354 the SCN1A-KO Model based on CRISPR/Cas9 Genome Editing Technology.
355 *Neuroscience* (2019) 1(398):1-11. doi: 10.1016/j.neuroscience.2018.11.052
356
- 357 21. Ingvar M, Söderfeldt B, Folbergrová J, Kalimo H, Olsson Y, Siesjö BK. Metabolic,
358 circulatory, and structural alterations in the rat brain induced by sustained
359 pentylenetetrazole seizures. *Epilepsia* (1984) 25(2):191-204. doi:
360 10.1111/j.1528-1157.1984.tb04176.x
361
- 362 22. Cornell-Bell AH, Finkbeiner SM, Cooper MS, Smith SJ. Glutamate induces
363 calcium waves in cultured astrocytes: long-range glial signaling. *Science* (1990)
364 247(4941):470-3. doi: 10.1126/science.1967852
365
- 366 23. Araque A, Parpura V, Sanzgiri RP, Haydon PG. Tripartite synapses: glia, the
367 unacknowledged partner. *Trends Neurosci* (1999) 22(5):208-15. doi:
368 10.1016/s0166-2236(98)01349-6
369
- 370 24. Rusakov DA, Zheng K, Henneberger C. Astrocytes as regulators of synaptic
371 function: a quest for the Ca²⁺ master key. *Neuroscientist* (2011) 17(5):513-23. doi:
372 10.1177/1073858410387304
373
- 374 25. Nedergaard M, Verkhratsky A. Artifact versus reality--how astrocytes contribute to
375 synaptic events. *Glia* (2012) 60(7):1013-23. doi: 10.1002/glia.22288
376
- 377 26. Hamilton NB, Attwell D. Do astrocytes really exocytose neurotransmitters? *Nat*

- 378 Rev Neurosci (2010) 11(4):227-38. doi: 10.1038/nrn2803. PMID: 20300101
- 379
- 380 27. Mahmoud S, Gharagozloo M, Simard C, Gris D. Astrocytes Maintain Glutamate
- 381 Homeostasis in the CNS by Controlling the Balance between Glutamate Uptake
- 382 and Release. Cells (2019) 8(2):184. doi: 10.3390/cells8020184
- 383
- 384 28. Aronica E, van Vliet EA, Mayboroda OA, Troost D, da Silva FH, Gorter JA.
- 385 Upregulation of metabotropic glutamate receptor subtype mGluR3 and mGluR5 in
- 386 reactive astrocytes in a rat model of mesial temporal lobe epilepsy. Eur J Neurosci
- 387 (2000) 12(7):2333-44. doi: 10.1046/j.1460-9568.2000.00131.x
- 388
- 389 29. Carmignoto G, Haydon PG. Astrocyte calcium signaling and epilepsy. Glia (2012)
- 390 60(8):1227-33. doi: 10.1002/glia.22318
- 391
- 392 30. Nikolic L, Nobili P, Shen W, Audinat E. Role of astrocyte purinergic signaling in
- 393 epilepsy. Glia (2020) 68(9):1677-1691. doi: 10.1002/glia.23747
- 394

395 Figure Legends

396 **Figure 1.** Spontaneous Ca^{2+} signaling in *Scn1a*^{+/-} astrocytes.

397 (A) Representative waveforms of spontaneous Ca^{2+} signaling in wild-type (WT) and

398 *Scn1a*^{+/-} astrocytes. Waveforms are shown relative to the baseline. (B) The waveform

399 expanded from a part of (A). (C) Mean of maximum relative intensity of spontaneous

400 Ca^{2+} signaling in WT and *Scn1a*^{+/-} astrocytes (WT: $19.9 \pm 1.8\%$, n = 123; *Scn1a*^{+/-}: 22.8

401 $\pm 1.3\%$, n = 179 from N = 5 cultures). (D) Representative differentiated waveforms of

402 spontaneous Ca^{2+} signaling in WT and *Scn1a*^{+/-} astrocytes. (E) Mean of the maximum

403 differential intensity of spontaneous Ca^{2+} signaling in WT and *Scn1a*^{+/-} astrocytes (WT:

404 $797.5 \pm 143.2 \Delta\text{Int}/\Delta\text{t}$, n = 98; *Scn1a*^{+/-}: $2796 \pm 481.3 \Delta\text{Int}/\Delta\text{t}$, n = 179 from N = 4

405 cultures).

406

407 **Figure 2.** ATP-induced Ca^{2+} signaling in *Scn1a*^{+/-} astrocytes.

408 (A) Representative waveforms of ATP-induced Ca^{2+} signaling in WT and *Scn1a*^{+/-}

409 astrocytes. Waveforms are shown relative to F/F₀. (B) The waveform expanded from a

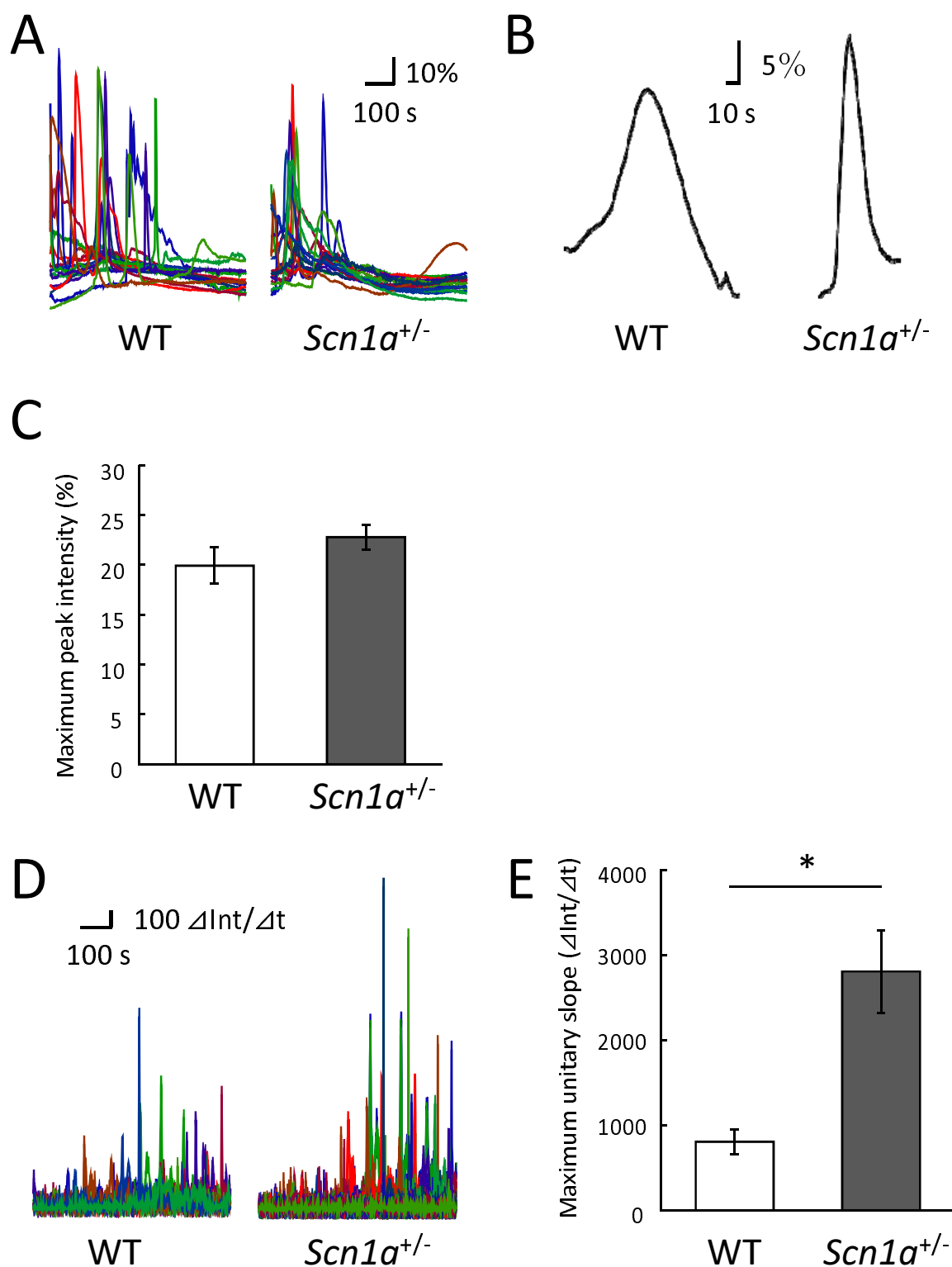
410 part of (A). (C) Mean of maximum relative peak intensity of ATP-induced Ca^{2+}

411 signaling in WT and *Scn1a*^{+/-} astrocytes (WT: $46.5 \pm 7.8\%$, n = 64; *Scn1a*^{+/-}: $86.4 \pm$

412 6.5% , n = 114 from N = 4 cultures). (D) Mean AUC of ATP-induced Ca^{2+} signaling in

413 WT and *Scn1a*^{+/-} astrocytes (WT: 49.5 ± 9.8 a.u., n = 74; *Scn1a*^{+/-}: 47.3 ± 4.9 a.u., n =
 414 125 from N = 4 cultures). (E) Representative differentiated waveforms of ATP-induced
 415 Ca²⁺ signaling in WT and *Scn1a*^{+/-} astrocytes. (F) Mean values of the maximum
 416 differential intensity of ATP-induced Ca²⁺ signaling in WT and *Scn1a*^{+/-} astrocytes (WT:
 417 601.1 ± 190.2 ΔInt/Δt, n = 63; *Scn1a*^{+/-}: 1154.5 ± 140.7 ΔInt/Δt, n = 114 from N =
 418 4 cultures).

Uchino et al., Fig 1



Uchino et al., Fig 2

